FISEVIER

Contents lists available at ScienceDirect

Optics Communications

journal homepage: www.elsevier.com/locate/optcom





Enhanced transmitter designs for indoor MIMO-VLC systems[☆]

Yinan Zhao a,b, Zhihong Zeng a,*, Hailin Cao a, Chen Chen a,*

- ^a School of Microelectronics and Communication Engineering, Chongqing University, Chongqing 400044, China
- b Department of Electrical and Computer Engineering, National University of Singapore, Singapore 117576, Singapore

ARTICLE INFO

Keywords: Visible light communication Multiple-input multiple-output Single transmitter partial coverage Distributed LED array

ABSTRACT

Multiple-input multiple-output (MIMO) technology, a fundamental element of 6G, has been widely implemented in visible light communication (VLC) systems. However, actual MIMO-VLC systems face significant challenges due to severe channel correlation. To tackle this issue, in this paper, we propose two enhanced transmitter designs for performance improvement of indoor MIMO-VLC systems, including single transmitter partial coverage (STPC) and enhanced STPC. For the STPC scheme, a single LED transmitter only needs to cover part of the receiving plane, instead of covering the whole receiving plane as in the conventional single transmitter full coverage (STFC) scheme. For the enhanced STPC scheme, each light-emitting diode (LED) is replaced with an LED subarray so as to further improve the system performance. Our simulation results reveal that the system performance is influenced by the LED array spacing, LED subarray spacing, and the LED semi-angle at half power. We identify the optimal combinations of these parameters to maximize the average achievable spectrum efficiency of the system. Notably, the STPC and Enhanced STPC schemes demonstrate increases in average achievable spectrum efficiency of 478.14% and 589.49%, respectively, compared to the benchmark STFC scheme.

1. Introduction

In recent years, the use and importance of wireless communication have increased significantly [1]. However, the available radio frequency (RF) bands are limited and are unlikely to provide significant new spectrum for wireless communications in the near future [2]. A promising alternative to RF is the use of indoor visible light communication (VLC) [3]. This is because a key advantage of VLC is that it allows lighting and communication to occur simultaneously, thereby saving power [4]. It is safe to deploy in areas where RF is difficult to use, e.g., underwater positioning and navigation in high-precision environments [5]. VLC can be fully utilized in environments where electromagnetic interference (EMI) is prohibited, such as in aircraft communication systems and hospital operating rooms [6–9]. Both the light source and receiver are reliable and scalable [10]. Therefore, VLC provides a promising solution for next-generation 6G mobile communications.

Owing to the limitations of off-the-shelf light emitting diode (LED)-based VLC, the modulation bandwidth is restricted to a few MHz [11]. Utilizing multiple-input multiple-output (MIMO) technology is one approach to overcome this limitation. The VLC data rate can be increased to several Gbit/s when using high spectral efficiency modulation schemes, especially MIMO techniques [12–17]. Due to the parallel

use of multiple transmitters and receivers, MIMO can improve spectral efficiency and reduce the bit error rate (BER). MIMO-VLC systems can also achieve high rate transmission without increasing transmit power and bandwidth [18]. Spatial multiplexing (SMP) is one of the most classical MIMO techniques. SMP achieves high data rates by exploiting multiplexing gains. To provide these gains, SMP requires sufficiently low channel correlation [19,20].

Single transmitter full coverage (STFC) is usually used in traditional MIMO solutions. However, actual MIMO-VLC systems suffer from severe channel correlation because of line-of-sight (LOS) transmission and the closely spaced photo-detectors (PDs). As a result, the multiplexing gain that can be achieved is not significant. In this regard, we propose the single transmitter partial coverage (STPC) scheme and the enhanced STPC scheme to a certain extent to alleviate this problem. In this study, numerical simulations are conducted to evaluate the performance of MIMO-VLC systems using the proposed schemes and further comparisons are made with the benchmark STFC scheme.

2. System model

The geometric setup of a general MIMO-VLC system is shown in Fig. 1(a), which is configured in a square room with a side length of l

E-mail addresses: 20211201011@cqu.edu.cn (Y. Zhao), zhihong.zeng@cqu.edu.cn (Z. Zeng), hailincao@cqu.edu.cn (H. Cao), c.chen@cqu.edu.cn (C. Chen).

This work was financially supported by the National Natural Science Foundation of China under Grant 62271091. The first author (Yinan Zhao) would like to express his gratitude to the financial support of the China Scholarship Council (CSC).

^{*} Corresponding authors.

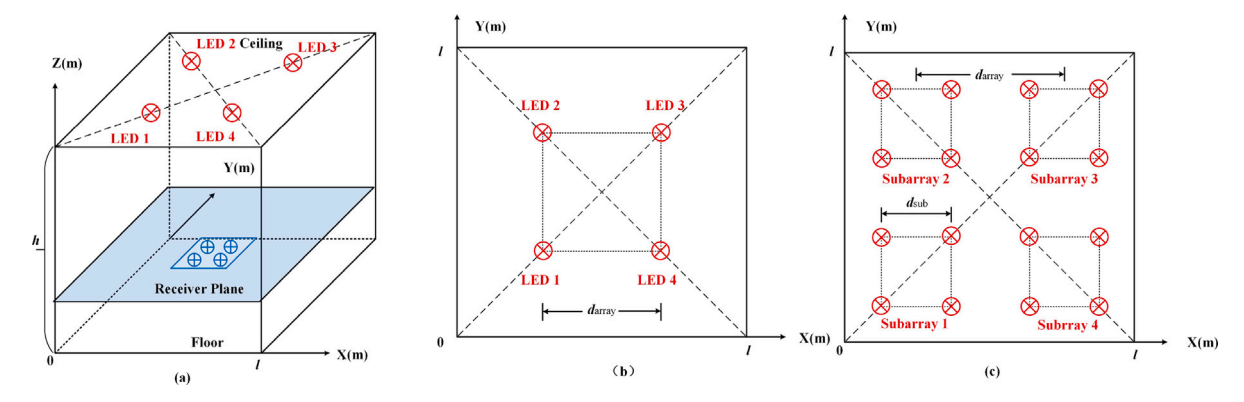


Fig. 1. (a) Geometric setup of a general MIMO-VLC system, (b) the transmitter setup for the STFC and STPC schemes, and (c) the transmitter setup for the enhanced STPC scheme.

and a vertical distance between the transmitter and the receiver of h. The MIMO-VLC system modulates the intensity of the optical power, transmits the signal through the LEDs, and then the signal reaches the receiver through the free space, where the receiver directly detects and recovers the transmitted information. The transmitter of the system consists of an array of LEDs, with the number of LEDs in the array denoted as $N_{\rm L}$. The receiver is equipped with $N_{\rm r}$ PDs. Therefore, the signal received at the receiver end can be expressed as

$$y = Hx + n, (1)$$

where $\mathbf{y} = \begin{bmatrix} y_1, \dots, y_{N_{\mathrm{r}}} \end{bmatrix}^{\mathrm{T}}$ is the received signal vector, $\mathbf{x} = \begin{bmatrix} x_1, \dots, x_{N_{\mathrm{t}}} \end{bmatrix}^{\mathrm{T}}$ is the signal vector at the transmitter, $\mathbf{n} = \begin{bmatrix} n_1, \dots, n_{N_{\mathrm{r}}} \end{bmatrix}^{\mathrm{T}}$ is the noise vector, and \mathbf{H} is the $N_{\mathrm{r}} \times N_{\mathrm{t}}$ dimensional channel transmission matrix, which is denoted as

$$\mathbf{H} = \begin{bmatrix} h_{1,1} & \cdots & h_{1,N_{t}} \\ \vdots & \ddots & \vdots \\ h_{N_{r},1} & \cdots & h_{N_{r},N_{t}} \end{bmatrix}, \tag{2}$$

where $h_{r,t}$ $(r=1,2,\ldots,N_r;t=1,2,\ldots,N_t)$ denotes the channel gain between the rth PD and the tth LED. If the channel matrix \mathbf{H} is full column rank (i.e., $(N_r \geq N_t)$, we can retrieve the signal vector x from the received signal via zero-forcing equalization as follows

$$\hat{\mathbf{x}} = \widetilde{\mathbf{H}}\mathbf{y} = \mathbf{x} + \widetilde{\mathbf{H}}\mathbf{n},\tag{3}$$

where $\widetilde{\mathbf{H}}$ denotes the pseudo inverse of \mathbf{H} , which is given by

$$\widetilde{\mathbf{H}} = (\mathbf{H}^* \mathbf{H})^{-1} \mathbf{H}^*, \tag{4}$$

where \mathbf{H}^* represents the conjugate transpose of \mathbf{H} . The noise is assumed to be real-valued additive white Gaussian noise (AWGN) with power $P_{\rm n}=N_0B$, where N_0 and B represent the noise power spectral density (PSD) and the signal bandwidth, respectively.

In indoor VLC systems, there are two main link models, LOS link and the non-line-of-sight (NLOS) link. In this paper, we only consider the LOS link, because it occupies more than 95% of the total received power [21]. It is assumed that the LED follows the Lambertian radiation pattern and the channel gain between the tth LED and tth PD is denoted by

$$h_{r,t} = \frac{(m+1)A_{d}}{2\pi d_{r,t}^{2}} \cos^{m}\left(\varphi_{r,t}\right) T\left(\theta_{r,t}\right) g\left(\theta_{r,t}\right) \cos\left(\theta_{r,t}\right), \tag{5}$$

where m is the Lambertian order of the LED and it is denoted as

$$m = -\frac{\ln 2}{\ln\left(\cos\boldsymbol{\phi}_{1/2}\right)},\tag{6}$$

where $\Phi_{1/2}$ is the semi-angle at half power of the LED; $d_{r,t}$ denotes the distance between the tth LED and the rth PD; $\varphi_{r,t}$ and $\theta_{r,t}$ denotes the irradiance angle and incident angle, respectively; $T\left(\theta_{r,t}\right)$ is the optical filter gain; $g\left(\theta_{r,t}\right)$ is the optical concentrator gain, where $g\left(\theta_{r,t}\right) = \frac{n^2}{\sin^2(\Psi)}$ with n and Ψ being the corresponding refractive index and the

field-of-view (FOV), respectively; $A_{\rm d}$ denotes the physical area of the PD.

In SMP-based indoor MIMO-VLC systems, different LEDs simultaneously transmit independent data streams and the signal-to-noise ratio (SNR) of the tth data stream can be calculated by

$$\gamma_{t} = \frac{P_{s}}{\sum_{r=1}^{N_{r}} (\widetilde{h}_{r,t})^{2} P_{n}} = \frac{\gamma_{0}}{\sum_{r=1}^{N_{r}} (\widetilde{h}_{r,t})^{2}},$$
(7)

where P_s is the transmitted optical power of each LED and γ_0 is the transmitted SNR, which is defined as $\gamma_0 = \frac{P_s}{P_{\rm n}}$, and $\widetilde{h}_{r,t}$ is the element in the rth row and tth column of $\widetilde{\bf H}$. The overall achievable spectrum efficiency of the $N_{\rm r} \times N_{\rm t}$ MIMO-VLC system using SMP can be obtained by

$$R = \sum_{t=1}^{N_t} \frac{1}{2} \log_2 \left(1 + \gamma_t \right)$$

$$= \frac{1}{2} \sum_{t=1}^{N_t} \log_2 \left(1 + \frac{\gamma_0}{\sum_{r=1}^{N_r} (\widetilde{h}_{r,t})^2} \right).$$
(8)

3. Single transmitter partial coverage

In this section, we present the details of the proposed STPC and enhanced STPC schemes, while comparing them with the classical STFC scheme. Fig. 1(b) shows the transmitter setup for the STFC scheme, where the LED array spacing, representing the distance between the adjacent LEDs in each array, is denoted as d_{array} . The STFC scheme refers to a classical MIMO-VLC system utilizing an array of LEDs where each LED fully covers the receiving plane as shown in Fig. 2(a). The diagram shows four circles representing the coverage areas of the LEDs. Each circle fully encompasses the receiving plane, illustrating that full coverage is achieved across the entire surface. However, the MIMO-VLC system with STFC suffers from severe channel correlation due to the LOS transmission and closely spaced PDs. Therefore, the STPC scheme is proposed in this study to overcome this issues. As shown in Fig. 1(b), the geometric setup of the STPC scheme is the same as the STFC scheme. Compared to the STFC scheme, each LED in the STPC scheme operates with a smaller semi-angle at half-power, resulting in partial coverage of the receiving plane. However, full coverage is still achieved through the combined effect of the LED array. Fig. 2(b) demonstrates this by depicting four circles, where each individual circle (representing the LED coverage area) does not fully cover the receiving plane, but the overall arrangement ensures complete coverage of the entire plane. Moreover, in this study, as shown in Fig. 1(c), by replacing each LED in the STFC scheme with a subarray of LEDs, we further propose the enhanced STPC scheme. The LED subarray spacing, representing the distance between the adjacent LEDs in each subarray, is denoted as d_{sub} . This approach seeks to deliver more uniform and controlled illumination across the receiving plane. The diagram for this scheme depicts

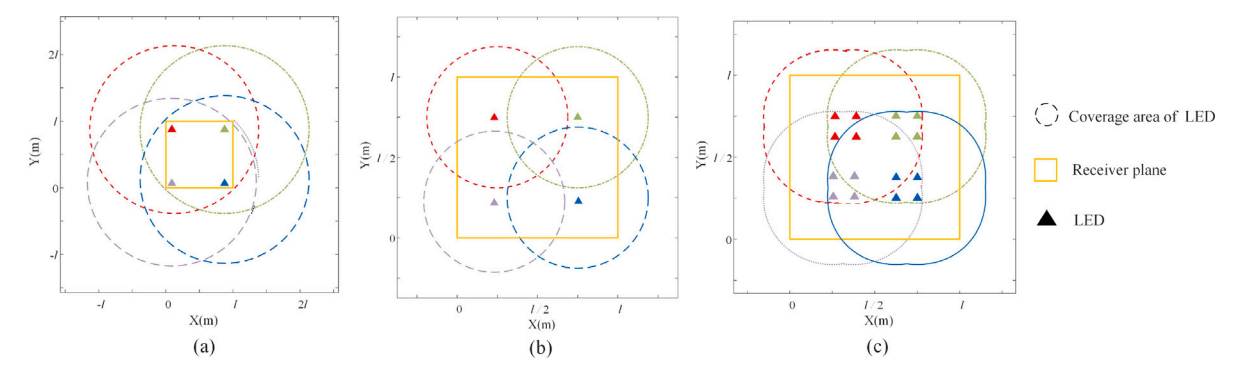


Fig. 2. Coverage diagrams of LEDs for (a) STFC, (b) STPC and (c) Enhanced STPC.

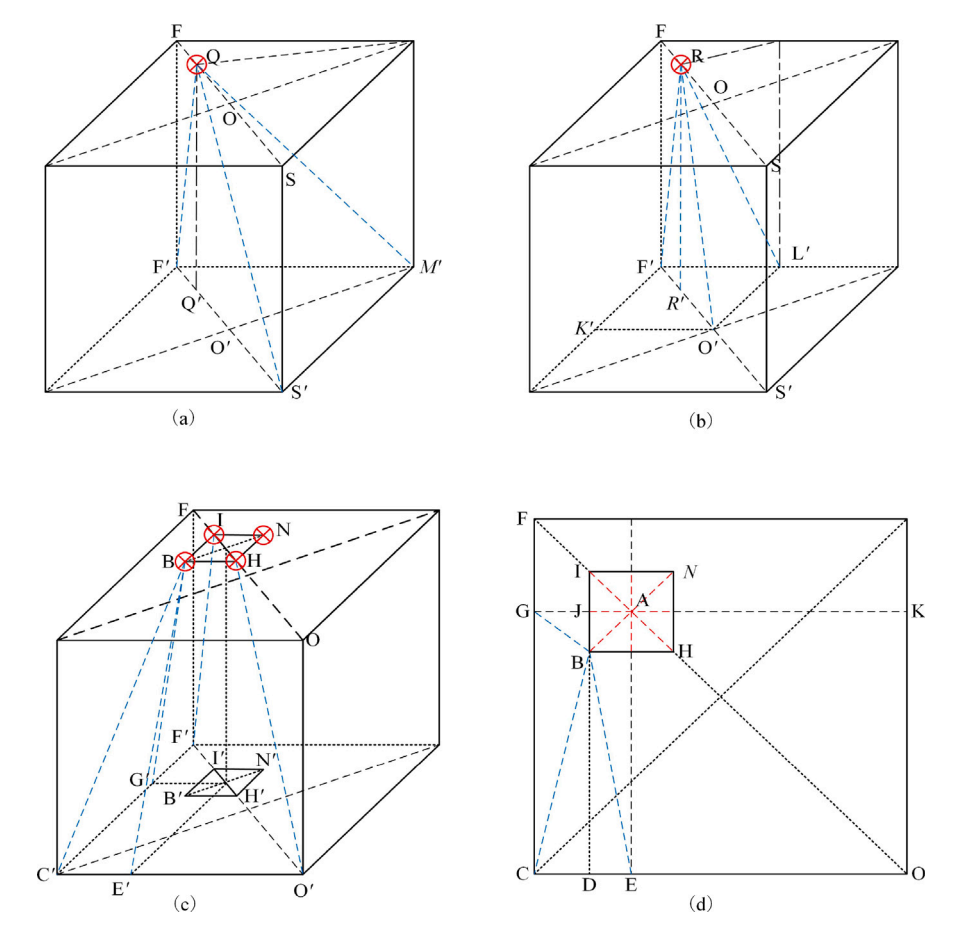


Fig. 3. Geometric schematic of the coverage area of the LED array for (a) STFC, (b) STPC, (c) enhanced STPC, and (d) the top view of the enhanced STPC scheme.

smaller, denser circles (representing the subarrays), which overlap to create a more granular and detailed coverage, ensuring comprehensive illumination of the receiving plane.

It is crucial to ensure that every point on the receiver plane receives adequate light from the LED array. Fig. 3 illustrates the geometric schematic of the coverage area of the LED array for various configurations, highlighting how different schemes affect the light distribution across the receiving surface. In the STFC scheme, each LED must cover the entire receiver plane. Given that both the room and the LED array are square and share the same center, diagonal symmetry can be leveraged for the analysis. Therefore, by verifying that the LED positioned at point Q in Fig. 3(a) can cover the entire receiver plane, we can infer that all LEDs placed symmetrically along the diagonals will cover the entire receiving surface effectively. As LED Q moves from point F to point O, it becomes evident that the entire receiver surface

is covered once points F', M', and S' are reached. Since these three points are covered if point S' is illuminated, to ensure full coverage, the semi-angle at half-power for the STFC scheme must satisfy the following conditions:

$$\Phi_{\text{STFC}} \ge \angle Q'QS' = \arctan \frac{Q'S'}{QQ'} = \frac{\sqrt{2}l + \sqrt{2}d_{\text{array}}}{2h}.$$
(9)

Considering the STPC scheme, each LED partially covers the receiving plane but ensures full coverage with the array of LEDs. As illustrated in Fig. 3(b), if the LED positioned at point R can cover points F', L', and O', then the entire receiver plane is covered. As LED Q moves from F to O, full coverage requires that during the first half of its movement, point O' must be covered, and during the second half, point F' must be

covered. Thus, the semi-angle at half-power for the STPC scheme must meet the following conditions:

$$\Phi_{\text{STPC}} \ge \begin{cases}
\angle R'RF' = \arctan \frac{R'F'}{RR'}, & 0 \le d_{\text{array}} \le \frac{l}{2} \\
\angle R'RO' = \arctan \frac{R'O'}{RR'}, & \frac{l}{2} \le d_{\text{array}} \le l
\end{cases}$$

$$= \begin{cases}
\frac{\sqrt{2}l - \sqrt{2}d_{\text{array}}}{2h}, & 0 \le d_{\text{array}} \le \frac{l}{2} \\
\frac{\sqrt{2}d_{\text{array}}}{2h}, & \frac{l}{2} \le d_{\text{array}} \le l
\end{cases}$$
(10)

In the enhanced STPC scheme, each subarray of LEDs partially covers the receiving plane, while the entire array of LED subarrays ensures full coverage. To clearly illustrate the coverage process from F to O, as shown in Fig. 3(c), we consider 1/4 of the room for geometric calculations. Given the symmetry in the array's coverage from F to O, we focus on the first half of the process. By leveraging geometric symmetry, we observe that when the LED at point I covers points F', G', E', and O', the entire receiving plane is adequately covered. The nearest LEDs responsible for covering these points are: LED I for point F', LED I for points I for point for the enhanced STPC scheme must meet the following conditions:

$$\Phi_{\text{E-STPC}} \ge \angle F' I I' = \arctan \frac{F' I'}{I I'}$$

$$= \frac{\sqrt{2}(l - d_{\text{array}} - d_{\text{sub}})}{h}.$$
(11)

To cover point G', it is required that

$$\Phi_{\text{E-STPC}} \ge \angle G' B B' = \arctan \frac{G' B'}{B B'}$$

$$= \frac{\sqrt{\left(l - d_{\text{array}} - d_{\text{sub}}\right)^2 + \left(d_{\text{sub}}\right)^2}}{2b}.$$
(12)

To ensure point E' is covered, it can be determined that

$$\Phi_{\text{E-STPC}} \ge \angle E'BB' = \arctan \frac{E'B'}{BB'}$$

$$= \frac{\sqrt{\left(d_{\text{array}} - d_{\text{sub}}\right)^2 + \left(d_{\text{sub}}\right)^2}}{2h}.$$
(13)

The point C' can be covered if

$$\Phi_{\text{E-STPC}} \ge \angle C'BB' = \arctan \frac{B'C'}{BB'}$$

$$= \frac{\sqrt{\left(d_{\text{array}} - d_{\text{sub}}\right)^2 + \left(l - d_{\text{array}} - d_{\text{sub}}\right)^2}}{2h}.$$
(14)

For the LED H to effectively cover point O', the following condition should be satisfied:

$$\Phi_{\text{E-STPC}} \ge \angle H'HO = \arctan \frac{H'O'}{HH'}$$

$$= \frac{\sqrt{2}d_{\text{array}} - \sqrt{2}d_{\text{sub}}}{2h}.$$
(15)

Additionally, to ensure that each LED in the array remains within the range from O to F, $d_{\rm array}$ needs to satisfy $d_{\rm array} \in (0, l)$. To ensure that there is always a certain distance between the LED subarrays, $d_{\rm sub} < \frac{d_{\rm array}}{2}$. To ensure that the LED in the subarray is always in the room, $d_{\rm sub} \le \frac{l-d_{\rm array}}{2}$.

4. Simulation results

In this study, we propose the STPC as well as enhanced STPC schemes and compare them with the traditional STFC scheme. This section evaluates the application of different schemes in a room with dimensions of $4\times4\times3$ m, featuring a square LED array centered on the ceiling. The height of the receiver plane is set at 1 m, with 1681 uniformly distributed receiver positions used to calculate the

Table 1
Simulation parameters.

Parameter	Value
Room dimension	$4 \text{ m} \times 4 \text{ m} \times 3 \text{ m}$
PD spacing	10 cm
Gain of optical filter, $T_{s}\left(\theta_{r,t}\right)$	1
Refractive index of optical lens, n	1.5
FOV of PD, Ψ	70°
Responsivity of PD, ρ	1 A/W
Height of receiving plane	1 m
Active area of PD, A_d	1 cm
Noise PSD, N_0	$10^{-22} A^2/Hz$
Modulation bandwidth, B	20 MHz

average achievable spectrum efficiency . Additionally, the semi-angle at half power of each LED $\Phi_{1/2}$ in the array is dynamically adjustable. Key parameters for this study are summarized in Table 1. Although a specific room configuration is considered in the simulations, the proposed STPC and enhanced STPC schemes are generally applicable to the room configuration with arbitrary sizes.

First, as shown in Fig. 4, we analyze the impact of the LED semiangle at half power ($\Phi_{1/2}$), array spacing (d_{array}), and subarray spacing (d_{sub}) on the performance of MIMO-VLC systems using the STFC, STPC, and enhanced STPC schemes. Our goal is to identify the optimal combination of these parameters to maximize the system's average achievable spectrum efficiency. The white pentagram marks the point of maximum achievable spectrum efficiency, while infeasible regions indicate areas where the matrix is not full rank, leading to invalid configurations. In Fig. 4(a), we observe the average achievable spectrum efficiency for varying $\Phi_{1/2}$ and d_{array} in the STFC scenario. As d_{array} increases, the average achievable spectrum efficiency fluctuates, peaking at $d_{array} = 3$ m and $\Phi_{1/2} = 68.33^{\circ}$. Fig. 4(b) presents the results for the STPC scenario, where the maximum achievable spectrum efficiency occurs with $d_{array} = 2$ m and $\Phi_{1/2} = 42.59^{\circ}$. In the enhanced STPC scheme, Fig. 4(c) shows that with an LED array spacing of 1.5 m, the maximum rate is achieved at $\Phi_{1/2} = 39^{\circ}$ and $d_{\text{sub}} = 0.48$ m. Similarly, Fig. 4(d) demonstrates that for an LED array spacing of 2 m, the highest rate is obtained with $\Phi_{1/2} = 46.3^{\circ}$ and $d_{\rm sub} = 0.2$ m. In this current work, the optimal parameters are obtained via numerical simulations. In our future work, we will consider the analytical derivation of the expressions for optimal $\Phi_{1/2}$, d_{array} and d_{sub} in the proposed STPC and enhanced STPC schemes.

Fig. 5 presents a performance comparison of MIMO-VLC systems utilizing STFC, STPC, and enhanced STPC schemes under varying array spacing. The relationship between the average achievable spectrum efficiency and array spacing for each scheme is depicted with the optimal values of $\Phi_{1/2}$ and $d_{\rm sub}$ selected for each point on the graph. As shown, the enhanced STPC scheme consistently outperforms the other two, while the STFC scheme always demonstrates the lowest performance. In the STFC case, the optimal array spacing occurs at $d_{\rm array}=3$ m, achieving an average spectrum efficiency of 2.8 bit/s/Hz. For the STPC scheme, the maximum average achievable spectrum efficiency of 13.2 bit/s/Hz is obtained at $d_{\rm array}=2$ m, reflecting a 478.1% improvement over the STFC scheme. The enhanced STPC scheme shows the highest performance, peaking at around 1.5 m, with a 589.5% improvement over the STFC scheme.

In Fig. 6, the performance of MIMO-VLC systems utilizing STFC, STPC, and enhanced STPC schemes are compared under different transmitted SNR levels. The enhanced STPC scheme consistently achieves the highest performance, with the rate increasing steadily as the SNR improves. The STPC scheme also demonstrates a steady increase but remains below the enhanced STPC. On the other hand, the STFC scheme shows the lowest performance, with the maximum achievable spectrum efficiency being the lowest among the three schemes across all SNR conditions. The main reason that the proposed STPC and enhanced STPC schemes can substantially improve the spectrum efficiency over

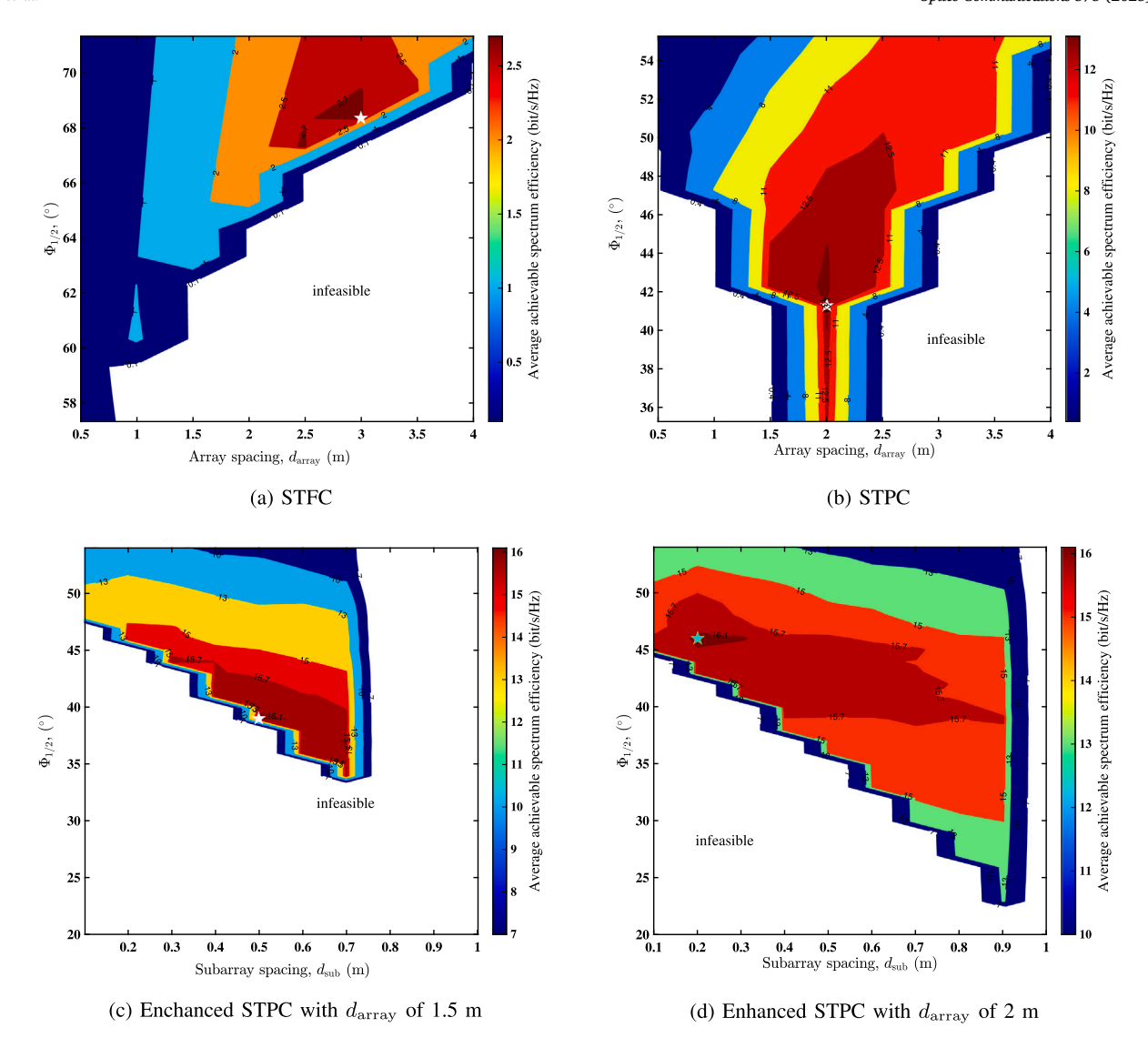


Fig. 4. Performance evaluation of STFC, STPC and enhanced STPC under varying semi-angle at half power of LED $\Phi_{1/2}$, the array spacing d_{array} , and the subarray spacing d_{sub} .

the conventional STFC scheme is that they can efficiently mitigate the channel correlation of MIMO transmission with a much reduced LED semi-angle at half power.

5. Conclusion

In this paper, we propose and analyze two enhanced transmitter designs including STPC and enhanced STPC schemes for MIMO-VLC systems. To achieve the maximum spectrum efficiency, we optimize the LED semi-angle at half power ($\Phi_{1/2}$), array spacing ($d_{\rm array}$), and subarray spacing ($d_{\rm sub}$) for each scheme. The optimal combinations of these parameters are identified via numerical simulations. We demonstrate that the proposed STPC and enhanced STPC schemes significantly outperform the traditional STFC scheme. More specifically, the enhanced STPC scheme exhibits the highest performance among the three, achieving a 589.5% improvement over the STFC scheme, achieves a 478.1% improvement over the STFC scheme. Therefore, the proposed enhanced transmitter designs can be promising for practical MIMO-VLC systems.

CRediT authorship contribution statement

Yinan Zhao: Writing – original draft, Visualization, Validation, Software, Project administration, Data curation. Zhihong Zeng: Writing – review & editing, Writing – original draft, Validation, Supervision, Software, Resources, Methodology, Investigation, Formal analysis, Conceptualization. Hailin Cao: Writing – review & editing, Supervision, Software. Chen Chen: Writing – review & editing, Supervision, Methodology, Funding acquisition.

Declaration of competing interest

The authors declare that they have no known competing financial interests or personal relationships that could have appeared to influence the work reported in this paper.

Data availability

No data was used for the research described in the article.

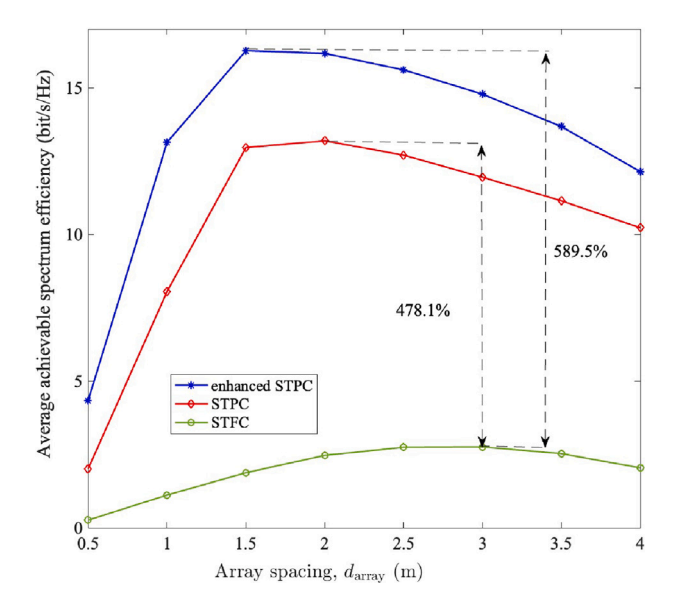


Fig. 5. Average achievable spectrum efficiency vs. LED array spacing.

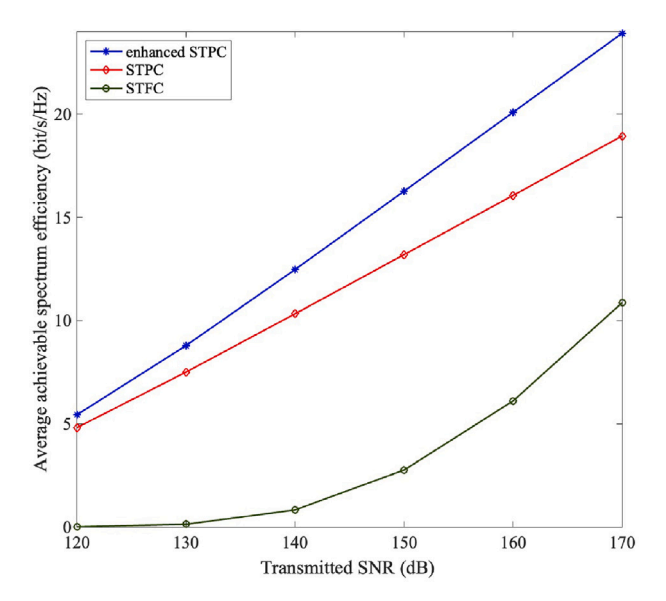


Fig. 6. Average achievable spectrum efficiency vs. transmitted SNR.

References

 J. Chapin, W. Lehr, Mobile broadband growth, spectrum scarcity, and sustainable competition, in: Proceedings of the 39th Research Conference on Communication, Information, and Internet Policy, TPRC, 2011.

- [2] H.C. Nguyen, I. Rodriguez, T.B. Sorensen, L.L. Sanchez, I. Kovacs, P. Mogensen, An empirical study of urban macro propagation at 10, 18 and 28 GHz, in: IEEE Vehicular Technology Conference, VTC Spring, 2016, pp. 1–5.
- [3] C.-H. Yeh, L.-Y. Wei, C.-W. Chow, Using a single VCSEL source employing OFDM downstream signal and remodulated OOK upstream signal for bi-directional visible light communications, Sci. Rep. 7 (1) (2017) 1–6.
- [4] R. Mitra, V. Bhatia, Precoding technique for ill-conditioned massive MIMO-VLC system, in: IEEE Vehicular Technology Conference, VTC Spring, 2018.
- [5] Y. Zhao, C. Chen, X. Zhong, H. Cao, M. Liu, B. Lin, S. Savović, Enhancing OFDM with index modulation using heuristic geometric constellation shaping and generalized interleaving for underwater VLC, Opt. Express 32 (8) (2024) 13720-13732
- [6] C. Wang, H.-Y. Yu, Y.-J. Zhu, A long distance underwater visible light communication system with single photon avalanche diode, IEEE Photonics J. 8 (5) (2016) 1-11.
- [7] H.-H. Lu, C.-Y. Li, H.-H. Lin, W.-S. Tsai, C.-A. Chu, B.-R. Chen, C.-J. Wu, An 8 m/9.6 Gbps underwater wireless optical communication system, IEEE Photonics J. 8 (5) (2016) 1–7.
- [8] C.-W. Hsu, J.-T. Wu, H.-Y. Wang, C.-W. Chow, C.-H. Lee, M.-T. Chu, C.-H. Yeh, Visible light positioning and lighting based on identity positioning and RF carrier allocation technique using a solar cell receiver, IEEE Photonics J. 8 (4) (2016) 1–7
- [9] C. Jenila, R.K. Jeyachitra, Green indoor optical wireless communication systems: Pathway towards pervasive deployment, Digit. Commun. Netw. 7 (3) (2021) 410–444.
- [10] P. Fahamuel, J. Thompson, H. Haas, Improved indoor VLC MIMO channel capacity using mobile receiver with angular diversity detectors, in: IEEE Global Communications Conference, 2014, pp. 2060–2065.
- [11] Z. Wang, J. Zhang, Z. He, N. Chi, Decision feedback Kurtosis minimum crosstalk mitigation in super-Nyquist multiband CAP systems, J. Lightwave Technol. 39 (21) (2021) 6774–6785.
- [12] C.-H. Yeh, H.-Y. Chen, C.-W. Chow, Y.-L. Liu, Utilization of multi-band OFDM modulation to increase traffic rate of phosphor-LED wireless VLC, Opt. Express 23 (2) (2015) 1133–1138.
- [13] M. Zhang, M. Shi, F. Wang, J. Zhao, Y. Zhou, Z. Wang, N. Chi, 4.05-Gb/s RGB LED-based VLC system utilizing PS-Manchester coded Nyquist PAM-8 modulation and hybrid time-frequency domain equalization, in: Optical Fiber Communication Conference, 2017, pp. W2A–42.
- [14] C.-W. Hsu, C.-W. Chow, I.-C. Lu, Y.-L. Liu, C.-H. Yeh, Y. Liu, High speed imaging 3×3 MIMO phosphor white-light LED-based visible light communication system, IEEE Photonics J. 8 (6) (2016) 1–6.
- [15] C. Yeh, H. Chen, Y. Liu, C.W. Chow, Polarization-multiplexed 2×2 phosphor-LED wireless light communication without using analog equalization and optical blue filter, Opt. Commun. 334 (2015) 8–11.
- [16] X. Zhong, C. Chen, Y. Zhao, M. Liu, C. He, H. Haas, Dual-mode spatial index modulation for MIMO-OWC, Opt. Lett. 49 (2) (2024) 334–337.
- [17] Y. Zhao, C. Chen, L. Zeng, M. Liu, Fully generalized optical spatial modulation, in: Opto-Electronics and Communications Conference, OECC, 2023, pp. 1–4.
- [18] P.F. Mmbaga, J. Thompson, H. Haas, Performance analysis of indoor diffuse VLC MIMO channels using angular diversity detectors, J. Lightwave Technol. 34 (4) (2015) 1254–1266.
- [19] T. Fath, H. Haas, Performance comparison of MIMO techniques for optical wireless communications in indoor environments, IEEE Trans. Commun. 61 (2) (2012) 733–742.
- [20] X. Zhong, C. Chen, W. Wen, M. Liu, H.Y. Fu, H. Haas, Optimization of surface configuration in IRS-aided MIMO-VLC: A BER minimization approach, IEEE Photonics J. 16 (3) (2024) 7301712.
- [21] T. Pham, A.T. Pham, Cooperation strategies and optimal precoding design for multi-user multi-cell VLC networks, in: IEEE Global Communications Conference, 2018.